RESEARCH ARTICLE

MOLECULAR BIOLOGY

RNA editing restricts hyperactive ciliary kinases

Dongdong Li[1234], Yufan Liu[1234], Peishan Yi[1234], Zhiwen Zhu[1234], Wei Li[5], Qiangfeng Cliff Zhang[1267], Jin Billy Li[8], Guangshuo Ou[1234]*

Protein kinase activity must be precisely regulated, but how a cell governs hyperactive kinases remains unclear. In this study, we generated a constitutively active mitogen-activated protein kinase DYF-5 (DYF-5CA) in *Caenorhabditis elegans* that disrupted sensory cilia. Genetic suppressor screens identified that mutations of ADR-2, an RNA adenosine deaminase, rescued ciliary phenotypes of *dyf-5CA*. We found that *dyf-5CA* animals abnormally transcribed antisense RNAs that pair with *dyf-5CA* messenger RNA (mRNA) to form double-stranded RNA, recruiting ADR-2 to edit the region ectopically. RNA editing impaired *dyf-5CA* mRNA splicing, and the resultant intron retentions blocked DYF-5CA protein translation and activated nonsense-mediated *dyf-5CA* mRNA decay. The kinase RNA editing requires kinase hyperactivity. The similar RNA editing–dependent feedback regulation restricted the other ciliary kinases NEKL-4/NEK10 and DYF-18/CCRK, which suggests a widespread mechanism that underlies kinase regulation.

Protein kinases mediate signal transduction and regulate fundamental cellular processes in eukaryotic cells. The catalytic activity of kinases must be stringently controlled, and its dysregulation leads to developmental defects, metabolic disorders, and cancer (*1*, *2*). Although loss-of-function kinase mutations have been extensively studied, gain-of-function mutations are less understood. Kinase hyperactivities have been described in many disease conditions, such as the constitutively active BCR-ABL1 tyrosine kinase in chronic myelogenous leukemia and BRAF serine/threonine kinase in malignant melanomas (*1*). Potent kinase inhibitors treat cancer effectively; however, tumors inevitably develop drug resistance and circumvent kinase inhibition by activating alternative pathways that perpetuate cell proliferation (*3*). Therefore, it is crucial to understand how an organism regulates hyperactive kinases.

We studied male germ cell–associated kinase (Mak), an evolutionarily conserved mitogen-activated protein kinase (MAPK). Mak localizes at the ciliary tip to restrict cilia elongation (*2*, *4*, *5*). Cilia are microtubule-based organelles essential for cell motility and sensory signaling, and ciliary defects cause more than 35 ciliopathies (*6*). The loss of Mak orthologs results in abnormally long cilia and leads to retinitis pigmentosa (*2*, *4*, *5*, *7*, *8*). By contrast, overexpression of mammalian Mak or *Caenorhabditis elegans* genomic DNA (gDNA) encoding the Mak ortholog DYF-5 inhibits ciliogenesis (*2*, *5*), which indicates that an optimal Mak/DYF-5 activity is essential. The MAPK superfamily contains a canonical TxY motif in the activation T-loop, phosphorylation of the threonine (pThr) residue activates the kinase, and glutamate can be a phosphomimetic pThr (*9*, *10*).

[1]Tsinghua-Peking Center for Life Sciences, Tsinghua University, Beijing, China. [2]Beijing Frontier Research Center for Biological Structure, Tsinghua University, Beijing, China. [3]McGovern Institute for Brain Research, Tsinghua University, Beijing, China. [4]School of Life Sciences and MOE Key Laboratory for Protein Science, Tsinghua University, Beijing, China. [5]School of Medicine, Tsinghua University, Beijing, China. [6]MOE Key Laboratory of Bioinformatics, School of Life Sciences, Tsinghua University, Beijing, China. [7]Center for Synthetic and Systems Biology, Tsinghua University, Beijing, China. [8]Department of Genetics, Stanford University School of Medicine, Stanford, CA, USA.
*Corresponding author. Email: guangshuoou@tsinghua.edu.cn

Results

A constitutively active DYF-5 kinase disrupted cilia

We first established that substitution of Thr^{164} with glutamate (T164E) in the TxY motif of DYF-5 leads to constitutive kinase activation in vitro. DYF-5(T164E) phosphorylated an intraflagellar transport (IFT) protein IFT-74, whereas wild-type (WT) DYF-5 did not (fig. S1, A to D), demonstrating that the substitution produced a constitutively active DYF-5 kinase (hereafter DYF-5CA). We then generated a T164E *dyf-5CA* knock-in animal in *C. elegans* (Fig. 1A and fig. S2, A and B). The *dyf-5CA* mutant (n > 200) exhibited normal morphology, viability, and growth rates comparable with those of the WT N2 strain. However, 87% of *dyf-5CA* worms (n = 150) could not use their sensory cilia to uptake fluorescence dye 1,1′-dioctadecyl-3,3,3′,3′-tetramethylindocarbocyanine perchlorate from the medium (Dyf) (Fig. 1B and fig. S2C), indicating an impaired ciliary function and integrity (*11*). To visualize IFT and cilia, we introduced a green fluorescence protein (GFP)–tagged IFT52/OSM-6 into *dyf-5CA*. In contrast to the bidirectional motility of OSM-6::GFP in WT cilia (*12*), no IFT was detectable from the distal ciliary segments of *dyf-5CA* (n > 20 animals), in which the OSM-6::GFP fluorescence formed aggregates (Fig. 1, C and D, and fig. S3, A and C to E).

The *dyf-5CA* animals developed abnormally elongated cilia, resembling the long cilia defect in the *dyf-5(mn400)* null allele (Fig. 1, B and D, and fig. S3B) but opposite to the truncated cilia phenotype when *dyf-5* gDNA was overexpressed (*2*). None of the *dyf-5CA* heterozygotes showed ciliary defects (n > 50 examined heterozygotes), and expression of the *dyf-5* cDNA in ciliated neurons fully rescued ciliary phenotypes in *dyf-5CA* (Fig. 1, B and D), indicating that *dyf-5CA* is a recessive loss-of-function mutant. Expression of *dyf-5CA* cDNA did not disrupt cilia in WT but rescued ciliary defects in *dyf-5CA* mutants (Fig. 1B and fig. S2D). Thus, the DYF-5CA protein did not have a dominant-negative effect. The discrepancy between the in vitro kinase hyperactivity and the in vivo kinase-null phenotype suggests that a previously unrecognized mechanism may control DYF-5CA in a living organism.

RNA adenosine deaminase mutations rescued ciliary defects by DYF-5CA kinase

We performed a forward genetic suppressor screen for mutations that restore *dyf-5CA* cilia (fig. S4A) and isolated four suppressors, *cas506*, *cas517*, *cas518*, and *cas519*, which exhibited uptake of fluorescence dye like the WT (n = 100) (fig. S4, B and C). All four mutations were mapped to the deaminase domain of ADR-2, with *cas517* carrying a premature stop codon and the other three mutants carrying missense mutations (Fig. 1E and fig. S4, B and D). A deletion mutant of *adr-2(ok735)* that removes the entire double-stranded RNA (dsRNA) binding domain and most of the deaminase domain (Fig. 1E and fig. S4E) showed the same ciliary rescue effects on *dyf-5CA* mutant cilia (Fig. 1, B and D, and fig. S3B).

ADR-2 is an ortholog of human ADARB1 (adenosine deaminase acting on RNA B1, or ADAR2). It exhibits dsRNA adenosine deaminase activity, catalyzing the adenosine-to-inosine (A-to-I) RNA editing, which is interpreted by the ribosome as guanosine (*13*, *14*). The *C. elegans* genome encodes two ADARs: ADR-1 is catalytically inactive, and ADR-2 is the only active RNA deaminase. The *adr-2* deletion completely abolishes A-to-I editing (*15*–*17*). Although ADR-1 regulates the activity of ADR-2 (*15*), the *adr-1* deletion did not recover *dyf-5CA* cilia (fig. S4C). By contrast, the *adr-2* deletion reduced the ciliary aggregates of OSM-6::GFP and improved IFT in both amphid and phasmid cilia of *dyf-5CA* animals, albeit at a slower speed (Fig. 1D and fig. S3, A and C to E). None of the *adr-2* mutant alleles displayed ciliary defects (n > 100, for each genotype) (Fig. 1B and fig. S4C). We used a ciliated neuron-specific promoter, P*dyf-1*, to express *adr-2* cDNA in the

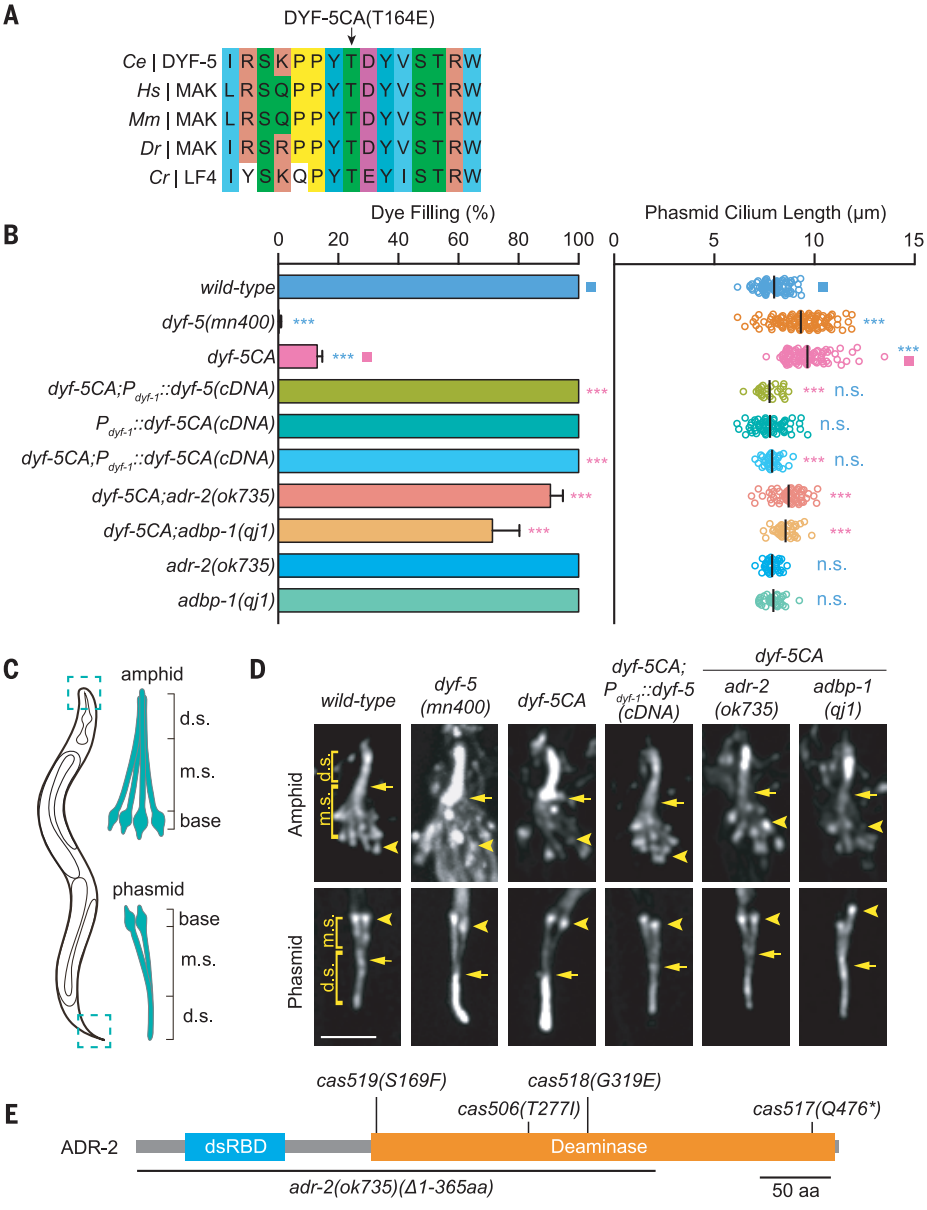

Fig. 1. ADR-2 mutations rescued ciliary defects in *dyf-5CA*. (**A**) Multi-sequence alignment of the *C. elegans* (Ce) DYF-5 kinase and its homologs in human (Hs), mouse (Mm), zebrafish (Dr), and *Chlamydomonas* (Cr). E, Glu; T, Thr. (**B**) Percentage of dye-filling positive animals in the indicated strains (mean ± SD) (left). N = 100 to 200. The cilium length of phasmid cilia (right, measured using the OSM-6::GFP fluorescence) is shown. N = 30 to 60. Statistical significance, compared with the control with a matching color code, is based on Student's *t* test; n.s., not significant, ***$P < 0.001$. (**C**) Schematic of the amphid and phasmid cilia. Dashed boxes are enlarged on the right. d.s., distal ciliary segment; m.s., middle segment. (**D**) Cilia in WT and mutants. Arrowheads indicate the ciliary base and transition zone, and arrows indicate junctions between the middle and distal segments. Scale bar, 5 μm. (**E**) ADR-2 protein domains. Amino acid changes and the deletion in *adr-2* mutant alleles are indicated. dsRBD, dsRNA binding domain. F, Phe; G, Gly; I, Ile; Q, Gln; S, Ser. Scale bar, 50 amino acids (aa).

dyf-5CA; adr-2 double mutant, which caused 75% of animals to develop the same ciliary defects that were observed in *dyf-5CA* animals (n = 300 transgenic animals) (fig. S4C), indicating that ADR-2 functions cell autonomously.

DYF-5CA caused aberrant RNA editing of the dyf-5CA *pre-mRNA*

We sought a mechanistic understanding between ADR-2 and DYF-5CA. An ADR-2::GFP reporter confirmed its nuclear localization (*13*) but did not reveal the ciliary localization of ADR-2 (fig. S5, A and B). Using GFP-affinity purification and mass spectrometry, we identified a known ADR-2 binding protein, ADBP-1, required for its deaminase activity (fig. S5C and data file S1) (*18*). The *adbp-1(qj1)* mutant recovered *dyf-5CA*'s ciliary defects (Fig. 1, B and D, and fig. S3, A to C), and GFP::ADBP-1 localized within nuclei, but not cilia (fig. S5D), suggesting that ADR-2 and ADBP-1 do not directly function in cilia but regulate DYF-5CA by their nuclear actions. Because ADR-2 and ADBP-1 are involved in small interfering RNA– and microRNA-associated pathways (*18*–*20*), we introduced RNA interference (RNAi) mutants into *dyf-5CA* but did not observe rescue effects (fig. S5E), indicating that the function of *adr-2* or *adbp-1* is independent of the RNAi machinery.

To understand ADR-2–based RNA editing in *dyf-5CA*, we implemented a comparative RNA-sequencing (RNA-seq) screen on WT, *dyf-5CA*, *adr-2*, and *dyf-5CA; adr-2* animals by using an established computational pipeline (*21*). WT animals had a total of 18,097 A-to-I editing sites, but RNA editing events were almost undetectable in *adr-2* or *adbp-1* (Fig. 2A, fig. S6A, and data file S2), which confirmed previous findings (*15*–*18*). In *dyf-5CA* animals, 12,871 sites that were edited in WT became unedited (Fig. 2A and data file S2). Because removing all the editing sites in the *dyf-5CA; adr-2* double mutant rescued *dyf-5CA*'s ciliary defects, we argue that these editing sites lost in *dyf-5CA* are not responsible for the phenotypes, although it is unclear why and how these sites were lost. The *dyf-5CA* animals unexpectedly acquired 1537 RNA editing sites, which were not detected in the WT and were lost in the *dyf-5CA; adr-2* (Fig. 2A and data file S2). Most of the identified RNA editing sites are located on chromosomes as clusters (*17*). We searched for the groups of ectopic editing sites and found that clustered sites were present in seven genes (fig. S6B and data file S2), including the *dyf-5CA* gene itself (Fig. 2B). The 269 editing

sites were distributed from the sixth exon to the seventh intron of *dyf-5CA* and occurred at frequencies of 10 to ~60% (Fig. 2C). By contrast, we did not detect any RNA editing sites in the *dyf-5* locus in other strains (Fig. 2B). Except for *dyf-5*, none of the other six genes were known to have ciliary functions.

We next investigated whether and to what extent the aberrant RNA editing clusters in *dyf-5CA* affect cilia. The sixth and seventh introns contain 130 editing sites, and the deletion of either intron or both in *dyf-5CA* animals rescued ciliary defects (Fig. 2D and figs. S2A and S7, A and B). The double intron deletion removed all the ectopic editing clusters in *dyf-5* exons (Fig. 2B). To rule out the effects of intron deletion on pre-mRNA, we synthesized the sixth and seventh introns by placing a noneditable T at all detected A-to-I editing sites. Replacing introns with noneditable sites rescued the ciliary phenotypes in *dyf-5CA* (Fig. 2D and figs. S2A and S7, B and C). Although other aberrantly gained or lost RNA editing sites may have biological functions under certain conditions, our data show that RNA editing sites in *dyf-5CA* are the primary cause for ciliary defects.

dyf-5CA *animals generated antisense transcripts in* dyf-5

Why does RNA editing occur specifically in this region? Because substrates of RNA editing enzymes are dsRNA (*13*), we examined whether long dsRNAs are formed intramolecularly at this locus but failed to identify any, which is consistent with lacking RNA editing at this

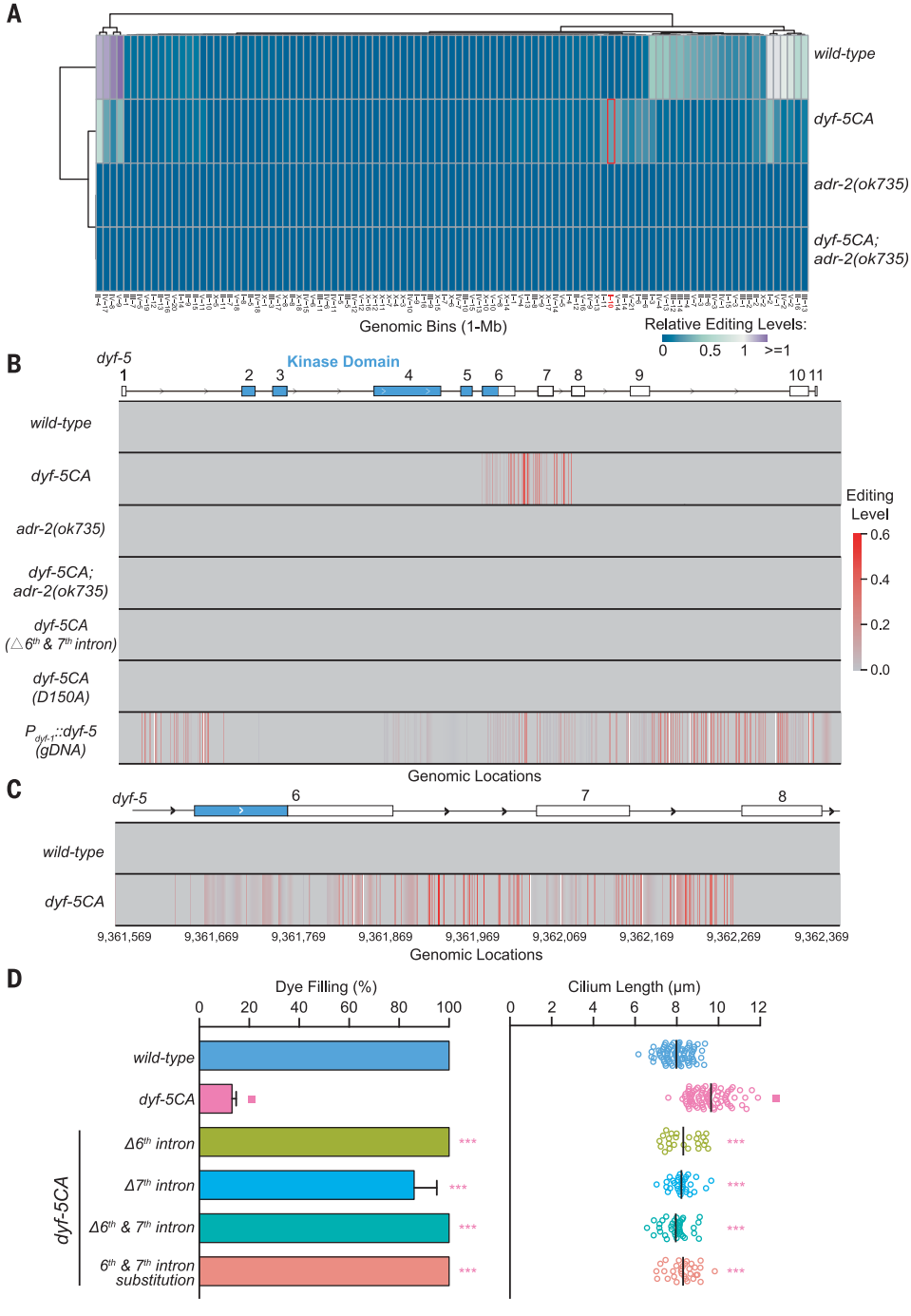

Fig. 2. ADR-2–dependent RNA editing clusters in *dyf-5CA*. (**A**) Heatmap and dendrogram of hierarchical clustering of editing sites using editing ratios among WT and mutants in different genomic bins (1-Mb tile) from RNA-seq data. Relative editing levels were used in hierarchical clustering. Each row corresponds to a sample. Each column represents the relative editing ratio in a genomic bin. Experiments were repeated three times with the similar results. The red box highlights the bin with the abnormally gained RNA editing sites of the *dyf-5* locus in *dyf-5CA*. (**B**) Representative RNA editing analysis at the *dyf-5* locus. Each row corresponds to a sample. Red lines represent RNA editing sites in the genomic locations of *dyf-5*, and the bar for editing level is shown on the right. Gene bodies are above; blue boxes show exons encoding the kinase domain. A, Ala; D, Asp. (**C**) Ectopic gain of RNA editing sites at the *dyf-5* locus in *dyf-5CA*. (**D**) Percentage of dye-filling (mean ± SD) positive animals in the indicated strains, n = 100 to 200 (left). Cilium length, n = 30 to 60 (right), is shown.

locus in the WT. We then investigated whether an antisense RNA was generated to form dsRNA with the *dyf-5CA* transcript subject to ADR-2 editing. Our strand-specific RNA-seq detected abundant antisense transcripts in *dyf-5CA* animals, starting from the seventh intron to the fourth exon of *dyf-5CA* and aligning with the region where aberrant RNA editing occurred (Fig. 3, A and B). Next, we examined whether the eighth intron of *dyf-5*, which is immediately upstream of the antisense transcripts, regulates antisense transcription. Although *dyf-5* cDNA expression did not cause ciliary abnormalities (Fig. 3C and figs. S2D and S8A), expression of *dyf-5* cDNA containing the sixth, seventh, and eighth introns, but not any individual intron, disrupted cilia (Fig. 3C). Conversely, *dyf-5* gDNA expression impaired cilia in an ADR-2–dependent manner (Fig. 3C and fig. S8A); however, expression of *dyf-5* gDNA that lacked the sixth, seventh, or eighth intron reduced the penetrance of ciliary defects (Fig. 3C). Consistently, *dyf-5* gDNA expression produced ectopic RNA editing clusters and antisense RNA transcription of *dyf-5*, which were not limited to the regions in *dyf-5CA* animals but spread to additional introns and exons of *dyf-5* (Figs. 2B and 3A), generating more profound effects than *dyf-5CA*. Deleting the eighth intron reduced the ciliary defects of *dyf-5CA* animals (Fig. 3C and fig. S7B), which demonstrates its contribution to ciliary defects. The incomplete penetrance of the eighth intron deletion suggests that other genomic region(s) might be involved. This intron may serve as a cryptic promoter for antisense transcription, and future studies will need to identify the additional cis-regulatory elements and the corresponding trans factor(s).

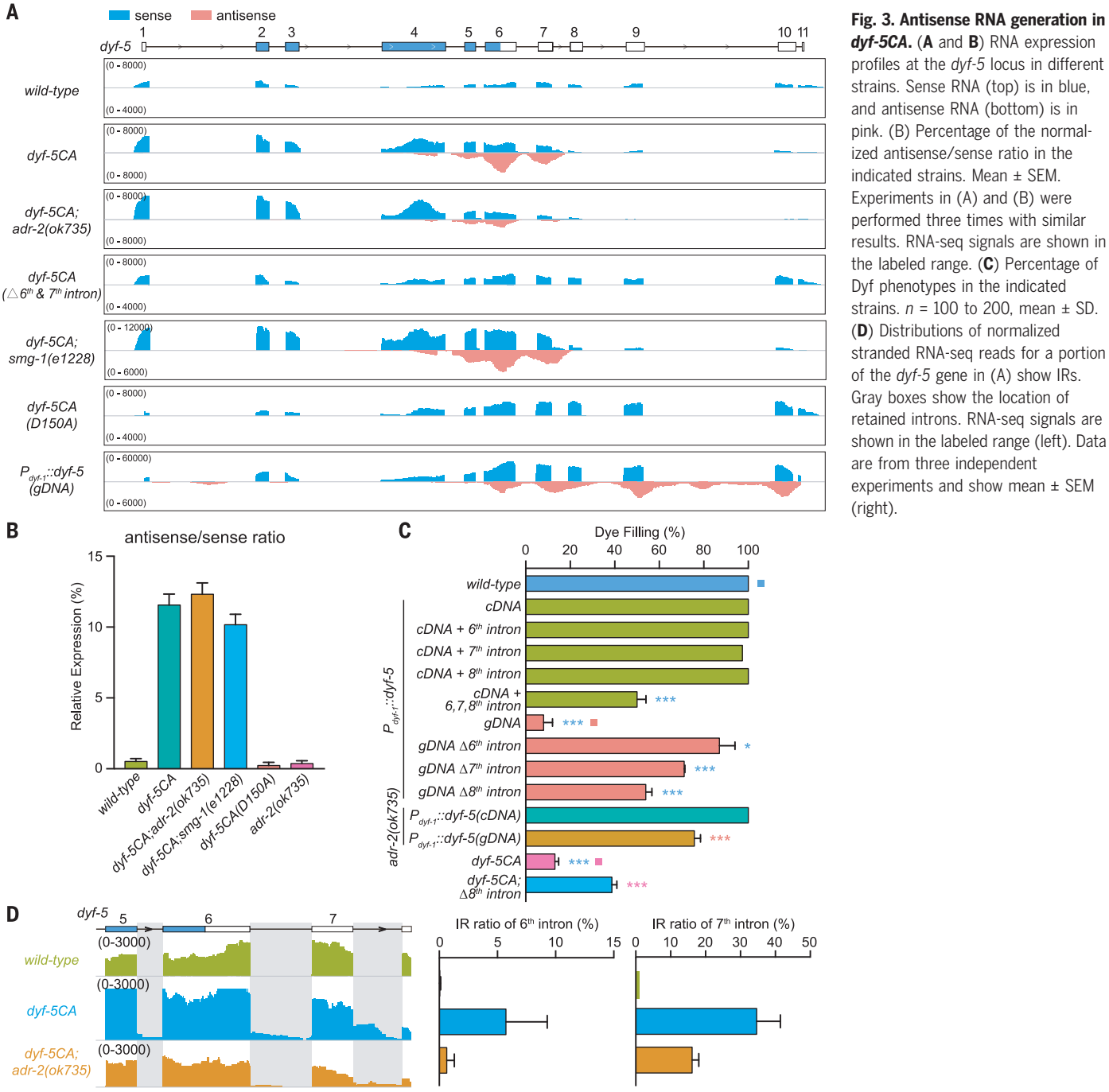

Fig. 3. Antisense RNA generation in *dyf-5CA*. (**A** and **B**) RNA expression profiles at the *dyf-5* locus in different strains. Sense RNA (top) is in blue, and antisense RNA (bottom) is in pink. (B) Percentage of the normalized antisense/sense ratio in the indicated strains. Mean ± SEM. Experiments in (A) and (B) were performed three times with similar results. RNA-seq signals are shown in the labeled range. (**C**) Percentage of Dyf phenotypes in the indicated strains. *n* = 100 to 200, mean ± SD. (**D**) Distributions of normalized stranded RNA-seq reads for a portion of the *dyf-5* gene in (A) show IRs. Gray boxes show the location of retained introns. RNA-seq signals are shown in the labeled range (left). Data are from three independent experiments and show mean ± SEM (right).

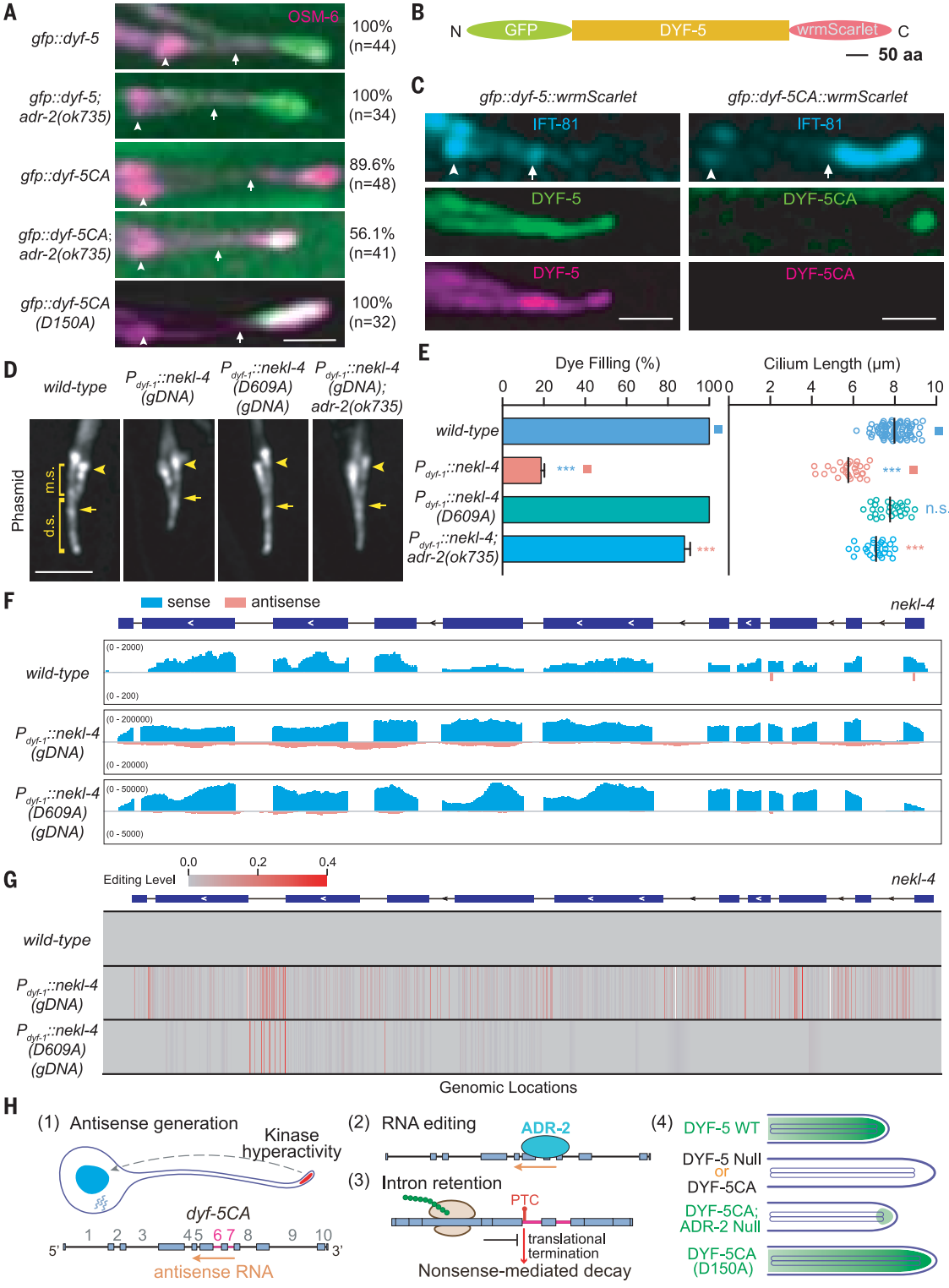

Fig. 4. DYF-5CA protein production and a working model. (**A**) Localization of GFP::DYF-5 or GFP::DYF-5CA with different genotypes. OSM-6::mCherry marks cilia. Percentages of DYF-5 localization patterns are indicated. (**B**) Schematic of *gfp::dyf-5::wrmScarlet* knock-in allele. Scale bar, 50 amino acids. (**C**) Localization of GFP::DYF-5::wrmScarlet (left) or GFP::DYF-5CA::wrmScarlet (right) in phasmid cilia. The blue fluorescence protein (BFP)–tagged IFT-81 labels cilia. Scale bars, (A) and (C), 2.5 μm. (**D**) Ciliary defects in the *nekl-4* gDNA overexpressed animals. Scale bar, 5 μm. (**E**) Percentage of dye filling (mean ± SD)–positive animals, *n* = 100 to 200 (left). Cilium length, *n* = 20 to 40 (right). (**F**) Mapping profiles of sense and antisense RNA at *nekl-4* in the WT *nekl-4* (upper) or kinase-dead *nekl-4(D609A)* (lower) gDNA overexpression animals (sense reads, blue; antisense reads, pink). (**G**) RNA editing clusters at *nekl-4*. The bar for editing level is shown on the top. (**H**) Model summarizes how RNA editing restricts hyperactive ciliary kinases.

Impaired dyf-5CA *mRNA splicing blocked DYF-5CA kinase translation*

Whereas antisense transcripts resulted in promiscuous RNA editing in *dyf-5CA*, it is the RNA editing, but not the antisense transcripts, that caused ciliary defects because *dyf-5CA; adr-2* double mutants that retained antisense transcripts but lacked RNA editing restored their cilia (Fig. 3, A and B). Thus, we studied the molecular consequence that RNA editing conferred in *dyf-5CA*. The hyperediting of the sixth and the seventh exons changed 40.5% of the amino acids in this region. The sixth exon is located in the kinase domain, implying a possible down-regulation of kinase activity (fig. S7D). The sixth and the seventh introns in the *dyf-5CA* pre-mRNA were not sufficiently spliced out, causing intron retention (IR) (Fig. 3, A and D). Using IRFinder (*22*), we found that the sixth and seventh IR ratios are 5.7 and 34.6% in *dyf-5CA*, respectively (Fig. 3D). By contrast, IR ratios were reduced to 0.6 and 16% in the *dyf-5CA;adr-2* double mutant, indicating that RNA editing of the intron sequence may promote IR. The incomplete elimination of IR in *dyf-5CA;adr-2* double mutants suggests that other mechanisms may be involved. For example, RNA editing is known to occur cotranscriptionally in nascent RNAs (*23*), and the ectopic antisense RNA transcripts can form dsRNA to prevent the spliceosome from accessing the *dyf-5CA* pre-mRNA.

To examine kinase production, we fused GFP to DYF-5 at its N terminus in WT or *dyf-5CA* animals. DYF-5 localized in the WT or *adr-2* mutant cilia (100%, $n > 30$ animals) (Fig. 4A and fig. S8B); however, GFP fluorescence was barely detected from 89.6% of *gfp::dyf-5CA* animals (Fig. 4A and fig. S8C). In *gfp::dyf-5CA;adr-2* double mutants, the GFP::DYF-5CA signal increased, albeit at a lower level than the WT (Fig. 4A), indicating that a small amount of hyperactive kinase restored cilia. To further evaluate whether the loss of GFP::DYF-5CA resulted from translation blockade, we fused a red fluorescent protein gene (wrmScarlet, the Scarlet protein with worm codon optimization) to the C terminus of GFP::DYF-5 or GFP::DYF-5CA (Fig. 4B). The green and red fluorescence colocalized in all the *gfp::dyf-5::wrmScarlet* cilia ($n = 60$ animals) (Fig. 4C); however, only the faint green but no red fluorescence was visible from all the examined *gfp::dyf-5CA::wrmScarlet* animals ($n = 43$) (Fig. 4C), which implies premature translation termination. Furthermore, the GFP-tagged DYF-5 kinase domain (11 to 291 amino acids) was localized in the cell body and dendrite but not in cilia, whereas the C terminus of DYF-5 (292 to 489 amino acids) entered cilia (fig. S8, D to F), indicating that its C terminus targeted the kinase domain to cilia. Thus, the *dyf-5CA* mRNA confers substantial defects in DYF-5 protein synthesis and, at least, its C-terminal ciliary localization domain, which prevents the kinase from phosphorylating its ciliary substrates.

Nonsense-mediated dyf-5CA *mRNA decay*

We examined the fate of *dyf-5CA* mRNAs. The A-to-I RNA editing did not create a stop codon; however, the intron-retaining transcripts often contained a premature termination codon (PTC) (fig. S7E) and might be targeted for degradation by the nonsense-mediated mRNA decay (NMD) pathway (*24*). Therefore, we crossed *dyf-5CA* animals with NMD mutants, including *smg-1*, a critical kinase that mediates the phosphorylation of an RNA helicase UPF1, and *smg-3*, an ortholog of human UPF2 (*25*, *26*). The *dyf-5CA* transcripts in the *dyf-5CA; smg-1* double mutants became ~1.8-fold more abundant than in *dyf-5CA*, which was confirmed by using quantitative polymerase chain reaction (PCR) experiments (Fig. 3A and fig. S9A). *smg-1* or *smg-3* mutation, which did not affect WT cilia ($n > 100$), partially rescued the ciliary dye-filling defects of *dyf-5CA* (fig. S9B) and reduced IFT-particle aggregation (fig. S9, C to E), although *smg-1* mutation did not shorten the elongated cilia (fig. S9F). Blocking of NMD rescued the phenotype in Ullrich's disease by up-regulating the mRNA level of the mutant collagen subunit and forming a partially functional extracellular matrix (*27*). Likewise, the inhibition of NMD increases the *dyf-5CA* mRNA level, a small portion of which may translate into functional kinase, partially restoring *dyf-5CA* cilia.

RNA editing restricted two other ciliary kinases

To explore whether RNA editing restricts other kinases, we screened five kinases by overexpressing the kinase gDNA in WT. Two ciliary kinases, NEKL-4/NEK10 (never in mitosis kinase like) and DYF-18/CCRK (ortholog of human cyclin-dependent kinase 20) (*28*–*30*), when overexpressed, resulted in ciliary defects, aberrant antisense transcripts, and RNA editing on kinase pre-mRNA (Fig. 4, D to G, and fig. S10, A to D). *adr-2* deletion rescued the ciliary phenotypes in kinase overexpression (OE) animals (Fig. 4, D and E, and fig. S10, A and B), indicating that ciliary defects require RNA editing. However, we did not detect abnormalities in animal phenotypes, antisense transcripts, or RNA editing of the rest of the three cytoplasmic kinase OE strains, including the POLO kinase PLK-1, the AKT kinase family kinase AKT-1, and the adenosine monophosphate–activated protein kinase AAK-2 (fig. S11), suggesting that RNA editing may specifically regulate ciliary kinases.

Kinase hyperactivation caused aberrant RNA editing

We determined whether kinase hyperactivity or transgene overexpression caused ectopic RNA editing. Expression of a catalytic dead D609A mutation of NEKL-4 (*31*) did not disrupt cilia (Fig. 4, D and E) and did not generate aberrant antisense transcription or RNA editing (Fig. 4, F and G). Similarly, the catalytically dead DYF-18(D145A) OE did not show ciliary phenotypes (fig. S10, A and B). We detected antisense transcription and RNA editing at levels similar to those of DYF-18 OE animals (fig. S10, C and D). We speculate that DYF-18(D145A) overexpression might have a residual activity in vivo, triggering RNA editing, but could not impair cilia. Consistently, the same amount of gDNA transformation disrupted cilia in 82% of NEKL-4OE but in only 23% of DYF-18OE animals (Fig. 4, D and E, and fig. S10, A and B), which suggests that the ciliary structure might be more sensitive to up-regulated NEKL-4. Furthermore, the catalytically dead DYF-5(D150A) or DYF-5(K40A) (K40A, $Lys^{40} \rightarrow Ala$) (*32*) OE reduced the ciliary phenotype penetrance (fig. S12A), accompanying a reduction of aberrant antisense transcripts and RNA editing (fig. S12, B and C). Thus, kinase activity is a substantial cause for ciliary defects and abnormal RNA editing.

To overcome the limitation of using kinase overexpression as a proxy kinase hyperactivity, we introduced D150A in *dyf-5CA* animals (fig. S2A). DYF-5CA(D150A) protein was translated and correctly localized to cilia (fig. S12D), and *dyf-5CA(D150A)* animals did not generate any antisense transcript or RNA editing on *dyf-5* (Figs. 2B and 3, A and B), which indicated that aberrant antisense expression and RNA editing resulted from DYF-5CA hyperactivity rather than overexpression. Because of catalytic null, *dyf-5CA(D150A)* animals developed ectopically long cilia like *dyf-5* null (fig. S12D). These results support a direct contribution of kinase hyperactivity to aberrant antisense transcription and RNA editing. We suggest that transgene overexpression increased WT kinase levels, which up-regulates kinase activity, which in turn triggers antisense transcription and RNA editing of the native kinase locus.

Considering that ADR-2 is known to suppress transgene silencing through editing dsRNA that is produced from aberrant overlapping antisense transcription (*33*), ciliary phenotypes from kinase gDNA overexpression may involve transgene silencing. We introduced the *rde-1 (ne219)* and *rde-4(ne301)* mutant alleles defective in transgene silencing (*34*) into *dyf-5*, *nekl-4*, and *dyf-18* gDNA OE animals, but their ciliary phenotypes were not changed (fig. S12E), suggesting that transgene silencing may not be involved.

Transcription regulation of dyf-5CA *mRNA*

dyf-5CA animals have more RNA-seq reads in the first seven exons but fewer reads in the final four exons than that of WT (Fig. 3A). We compared the stability of the *dyf-5* transcripts in WT and *dyf-5CA* animals after treatment

with actinomycin D, which blocks transcription. *dyf-5* pre-mRNAs were degraded at a similar rate in both strains (fig. S13A), which suggests that DYF-5CA may not affect transcript stability. *dyf-5CA* animals abnormally transcribe antisense RNA from the fourth exon to the seventh intron of *dyf-5*; the resultant dsRNA may inhibit RNA polymerase II (Pol II) elongation (*35*). To assess the potential transcriptional changes, we performed RNA Pol II chromatin immunoprecipitation followed by sequencing chromatin immunoprecipitation–sequencing (ChIP-seq). Compared with WT, *dyf-5CA* animals increased Pol II occupancy in the third to eighth exon of *dyf-5* (fig. S13B). Similar increases were observed for the elongation-specific Pol II phosphorylated at serine 2 (fig. S13B). ChIP-seq of histone H3 trimethylation at Lys^{36} (H3K36me3) revealed increased H3K36me3 modifications in this region due to Pol II elongation and cotranscriptional deposition of H3K36me3 (fig. S13B). The increased densities indicate aberrantly high transcript elongation in the region and suggest that the lack of transcripts in the final few exons may result from transcription regulation. The *adr-2* deletion did not affect these densities in *dyf-5CA* (fig. S13B), which suggests that the increased occupancy may occur upstream or independent of RNA editing. By contrast, introducing D150A to *dyf-5CA* eliminates all the increased occupancy (fig. S13B), indicating that kinase hyperactivity causes abnormal transcription regulation.

Ciliary phenotypes in dyf-5CA *and* dyf-5 gOE *animals*

Why do *dyf-5CA* animals aberrantly elongate cilia but *dyf-5 gOE* worms shorten cilia? The absence of GFP fluorescence from *gfp::dyf-5CA* animals indicates that DYF-5CA protein is not produced, phenocopying the long cilia phenotype in *dyf-5* null. The *wrmScarlet::dyf-5 gOE* animals produced the wrmScarlet::DYF-5 fluorescence that was incorrectly distributed around the ciliary base (fig. S14, A, B, and G). Introducing *adr-2* null into *wrmScarlet::dyf-5 gOE* animals restored DYF-5 localization to the distal ciliary segments (fig. S14B) where DYF-5 is normally found, indicating that DYF-5 mislocalization owing to *dyf-5 gOE* is suppressed by the loss of ADR-2. Consistently, deletion of *adr-2* rescued the short cilia defects in *dyf-5 gOE* (fig. S14, C and G). Using quantitative fluorescence and quantitative real-time PCR experiments, we showed that the loss of ADR-2 does not affect the transgene expression level of *wrmScarlet::dyf-5 gOE* or *osm-6::gfpOE* (fig. S14, D and E), which indicates that ADR-2 does not regulate *dyf-5 gOE* phenotypes through promoting transgene expression. Because DYF-5 prevents cilia overgrowth (*2*), mislocalized DYF-5 at the ciliary base might have blocked cilia elongation in *dyf-5 gOE*. To test this possibility, we artificially targeted DYF-5 to the ciliary base by fusing *dyf-5* cDNA with a ciliary transition zone gene *mksr-2*. Indeed, *mksr-2::dyf-5cDNA OE* animals developed short cilia like that of *dyf-5 gOE* (fig. S14, C, F, and G); however, overexpressed DYF-5 protein from *dyf-5* cDNA correctly localized at the ciliary distal and did not impair cilia (fig. S14, B, C, and G). We suggest that as long as DYF-5 localizes at the correct place, it will not generate deleterious effects, even though its amount or activity might be higher than in WT animals. In *adr-2* mutants that have increased *dyf-5CA* levels but lose RNA editing, the full-length DYF-5CA proteins with the C-terminal localization domain can be produced and properly localize at the distal ciliary segments; therefore, no shortening of cilia was observed. We speculate that *dyf-5 gOE* animals expressed abundant *dyf-5* pre-mRNA, a portion of which, after RNA editing, may translate the DYF-5 kinase domain, incorrectly localizing around the ciliary base to inhibit cilia growth. By contrast, *dyf-5CA* animals expressed a much lower level of *dyf-5CA* pre-mRNA than *dyf-5 gOE*, and RNA editing may severely block DYF-5CA protein production, causing aberrant cilia elongation. If the *dyf-5CA* pre-mRNA increases under certain conditions, the animal may produce truncated DYF-5 protein that localizes at the ciliary base to inhibit cilia elongation.

Cilia-to-nuclei signaling

dyf-5CA animals exhibited higher levels of *dyf-5* mRNA than WT (Fig. 3A), which suggests negative transcriptional feedback so that the loss of DYF-5 up-regulates *dyf-5* expression. We found an up-regulation of other ciliary gene expressions in the *dyf-5CA* and *dyf-5 (mn400)* null allele and ciliary mutants that were defective in IFT-dynein CHE-3 and IFT-particle subunit DAF-10 (fig. S15 and data files S3 and S4). Flagella removal in *Chlamydomonas* caused a rapid transcription up-regulation of hundreds of flagellar-associated genes (*36*). Thus, a cell appears to sense whether cilia function or exist, and the "stressed" cilia may signal to the nucleus, requesting more ciliary proteins, which resembles the unfolded protein response (UPR) between the endoplasmic reticulum and the nucleus (*37*). Analogous to UPR regulation, an overphosphorylated ciliary protein of yet unknown identity may travel from *dyf-5CA* cilia into the nucleus to activate antisense transcription. This study describes a negative feedback loop in *dyf-5CA* animals. Given that cilia-to-nucleus signaling occurs in other ciliary mutants and deflagellated conditions, we speculate that the feedback loop elements may play roles in conditions beyond *dyf-5CA*. For example, WT worms that carry a mutation disabling the feedback loop (such as the intron substitution *dyf-5* allele in fig. S2A) might display phenotypes under certain stressful conditions.

Discussion

We propose a model through which RNA editing restricts the hyperactive DYF-5CA ciliary kinase (Fig. 4H): (i) In response to kinase hyperactivity, antisense RNAs are transcribed in nuclei and pair with the kinase pre-mRNA. (ii) The dsRNA recruits RNA deaminase to edit kinase pre-mRNA, which changes the kinase protein sequence and impairs kinase pre-mRNA splicing. (iii) The resultant IRs generate premature stop codons, which inhibit kinase translation and activate nonsense-mediated kinase mRNA decay. (iv) The loss of kinase production converts a biochemically hyperactive kinase to loss of function in vivo, phenocopying the kinase-null cilia. Considering that *dyf-5 gOE* generated more RNA editing sites on *dyf-5* locus than *dyf-5CA* (Fig. 2B), we suggest that kinase gRNA OE might involve additional regulation. However, the loss of RNA editing rescued ciliary defects under kinase gDNA OE conditions (Figs. 3C and 4, D and E, and fig. S10, A and B), underscoring the crucial role of RNA editing in safeguarding against the overactivation of kinases.

In addition to ciliary kinases, an increasing number of kinase mRNAs are hyperedited during disease progression. Examples include the protein kinase R during type I interferon responses and the CDK12 kinase mRNA from ovarian cancer cells (*38–40*). Although the mechanisms and impacts may differ from each of these RNAs, a parallel does emerge: RNA editing is linked to kinase hyperactivity. Recognizing this common linkage, we suggest that in response to physiological or pathological stimuli, RNA editing may target the kinase pre-mRNA, restricting kinase production and down-regulating its activity in vivo.

Our demonstration, in which suppression of RNA editing rescues ciliary defects caused by hyperactive kinases, connects cilia with other processes. Most of the ciliopathy genes are not ideal for drug development (*6*). We anticipate that the development of small molecules that target the pathways outside of cilia holds promise to devise strategies for the treatment of ciliopathies.

REFERENCES AND NOTES

1. P. Lahiry, A. Torkamani, N. J. Schork, R. A. Hegele, *Nat. Rev. Genet.* **11**, 60–74 (2010).
2. J. Burghoorn *et al.*, *Proc. Natl. Acad. Sci. U.S.A.* **104**, 7157–7162 (2007).
3. N. Vasan, J. Baselga, D. M. Hyman, *Nature* **575**, 299–309 (2019).
4. S. A. Berman, N. F. Wilson, N. A. Haas, P. A. Lefebvre, *Curr. Biol.* **13**, 1145–1149 (2003).
5. Y. Omori *et al.*, *Proc. Natl. Acad. Sci. U.S.A.* **107**, 22671–22676 (2010).
6. J. F. Reiter, M. R. Leroux, *Nat. Rev. Mol. Cell Biol.* **18**, 533–547 (2017).
7. R. K. Ozgül *et al.*, *Am. J. Hum. Genet.* **89**, 253–264 (2011).

8. B. A. Tucker *et al*., *Proc. Natl. Acad. Sci. U.S.A.* **108**, E569–E576 (2011).
9. P. D. Mace *et al*., *Nat. Commun.* **4**, 1681 (2013).
10. Z. Fu *et al*., *Mol. Cell. Biol.* **25**, 6047–6064 (2005).
11. L. A. Perkins, E. M. Hedgecock, J. N. Thomson, J. G. Culotti, *Dev. Biol.* **117**, 456–487 (1986).
12. G. Ou, O. E. Blacque, J. J. Snow, M. R. Leroux, J. M. Scholey, *Nature* **436**, 583–587 (2005).
13. K. Nishikura, *Nat. Rev. Mol. Cell Biol.* **17**, 83–96 (2016).
14. L. A. Tonkin *et al*., *EMBO J.* **21**, 6025–6035 (2002).
15. M. C. Washburn *et al*., *Cell Rep.* **6**, 599–607 (2014).
16. J. A. Arribere, H. Kuroyanagi, H. A. Hundley, *Genetics* **215**, 531–568 (2020).
17. H. Q. Zhao *et al*., *Genome Res.* **25**, 66–75 (2015).
18. H. Ohta, M. Fujiwara, Y. Ohshima, T. Ishihara, *Genetics* **180**, 785–796 (2008).
19. D. P. Reich, K. M. Tyc, B. L. Bass, *Genes Dev.* **32**, 271–282 (2018).
20. M. B. Warf, B. A. Shepherd, W. E. Johnson, B. L. Bass, *Genome Res.* **22**, 1488–1498 (2012).
21. F. Zhang, Y. Lu, S. Yan, Q. Xing, W. Tian, *Bioinformatics* **33**, 3538–3548 (2017).
22. R. Middleton *et al*., *Genome Biol.* **18**, 51 (2017).
23. J. Rodriguez, J. S. Menet, M. Rosbash, *Mol. Cell* **47**, 27–37 (2012).
24. T. Kurosaki, M. W. Popp, L. E. Maquat, *Nat. Rev. Mol. Cell Biol.* **20**, 406–420 (2019).
25. A. Grimson, S. O'Connor, C. L. Newman, P. Anderson, *Mol. Cell. Biol.* **24**, 7483–7490 (2004).
26. L. Johns, A. Grimson, S. L. Kuchma, C. L. Newman, P. Anderson, *Mol. Cell. Biol.* **27**, 5630–5638 (2007).
27. F. Usuki *et al*., *Proc. Natl. Acad. Sci. U.S.A.* **110**, 15037–15042 (2013).
28. R. R. Chivukula *et al*., *Nat. Med.* **26**, 244–251 (2020).
29. A. K. Maurya, T. Rogers, P. Sengupta, *Curr. Biol.* **29**, 1286–1300.e4 (2019).
30. K. M. Power *et al*., *PLOS Genet.* **16**, e1009052 (2020).
31. S. H. Schmidt *et al*., *Proc. Natl. Acad. Sci. U.S.A.* **116**, 14979–14988 (2019).
32. L. Xia *et al*., *J. Biol. Chem.* **277**, 35422–35433 (2002).
33. S. W. Knight, B. L. Bass, *Mol. Cell* **10**, 809–817 (2002).
34. H. Tabara, E. Yigit, H. Siomi, C. C. Mello, *Cell* **109**, 861–871 (2002).
35. V. Pelechano, L. M. Steinmetz, *Nat. Rev. Genet.* **14**, 880–893 (2013).
36. A. J. Albee *et al*., *G3* **3**, 979–991 (2013).
37. P. Walter, D. Ron, *Science* **334**, 1081–1086 (2011).
38. C. Calabrese *et al*., *Nature* **578**, 129–136 (2020).
39. H. Chung *et al*., *Cell* **172**, 811–824.e14 (2018).
40. J. J. Ishizuka *et al*., *Nature* **565**, 43–48 (2019).

ACKNOWLEDGMENTS

We thank J. Reiter, X. Yang, V. Ambros, D. Xue, Z. Lu, X. Shen, Y. Qi, S. Cai, and Y. Wang for discussion. **Funding:** This work was supported by the following funding programs: National Natural Science Foundation of China (grants 31991190, 31730052, 31525015, 31861143042, 31561130153, 31671444, and 31871352) and National Key R&D Program of China (2017YFA0503501, 2019YFA0508401, and 2017YFA0102900). **Author contributions:** D.L., P.Y., Z.Z., W.L., Q.C.Z., J.B.L., and G.O. conceived and designed the project. D.L., Z.Z., and P.Y. performed research; D.L. and Y.L. analyzed data; D.L., Z.Z., W.L., Q.C.Z., J.B.L., and G.O. wrote the paper. **Competing interests:** G.O., W.L., D.L., Z.Z., and P.Y. are inventors on patent application no. CN202110893049.4, submitted by Tsinghua University, that covers applications of RNA editing on genetic disorders that are associated with gain-of-function proteins. **Data and materials availability:** All data are available in the main text or supplementary materials. All sequencing data from this study have been submitted to the NCBI Sequence Read Archive (SRA; www.ncbi.nlm.nih.gov/sra) with BioProject accession number PRJNA655606.

SUPPLEMENTARY MATERIALS

science.sciencemag.org/content/373/6558/984/suppl/DC1
Materials and Methods
Figs. S1 to S15
Tables S1 to S5
References (*41*–*47*)
MDAR Reproducibility Checklist
Data S1 to S4

24 August 2020; resubmitted 1 April 2021
Accepted 16 July 2021
10.1126/science.abd8971

RNA editing restricts hyperactive ciliary kinases

Dongdong Li, Yufan Liu, Peishan Yi, Zhiwen Zhu, Wei Li, Qiangfeng Cliff Zhang, Jin Billy Li and Guangshuo Ou

Science **373** (6558), 984-991.
DOI: 10.1126/science.abd8971

RNA editing restricts ciliary kinases

Ciliary kinases are essential for cilia formation and function but it remains unknown how their activities are regulated in vivo. Li *et al.* created roundworm animal models carrying hyperactive ciliary kinases that disrupt cilia. Their genetic suppressor screens revealed that loss of an RNA adenosine deaminase that catalyzes adenosine-to-inosine (A-to-I) RNA editing rescued ciliary abnormalities. They found that kinase hyperactivation caused this RNA adenosine deaminase to edit kinase RNA and impair kinase RNA splicing and translation, thereby downregulating ciliary kinases from nuclei. These results suggest that ciliopathies may be treated by targeting the pathways outside of cilia.

Science, abd8971, this issue p. 984